

NUMERICAL STUDY OF CONTROLLING BLOOD FLOW THROUGH A STENOSED ARTERY USING POWER-LAW FLUID

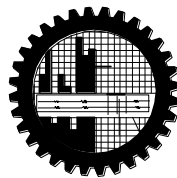
by

MD. AMZAD HOSSAIN

Student No. 1017092512F

Registration No. 1017092512, Session: October 2017

MASTER OF SCIENCE
IN
MATHEMATICS



Department of Mathematics
Bangladesh University of Engineering and Technology (BUET)
Dhaka-1000
October, 2019

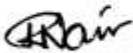
The thesis titled


NUMERICAL STUDY OF CONTROLLING BLOOD FLOW THROUGH A STENOSED ARTERY USING POWER-LAW FLUID


Submitted by
MD. AMZAD HOSSAIN

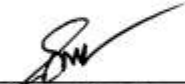
Student No. 1017092512F, Registration No. 1017092512, Session: October, 2017, a full time student of M. Sc. Mathematics has been accepted as satisfactory in partial fulfillment for the degree of Master of Science in Mathematics on 1st October, 2019.

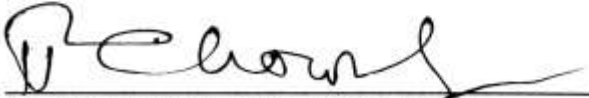
BOARD OF EXAMINERS

1. 

Dr. Rehana Nasrin
Professor
Department of Mathematics
BUET, Dhaka-1000
Chairman
(Supervisor)
2. 

Head
Department of Mathematics
BUET, Dhaka-1000
Member
(Ex-Officio)
3. 

Dr. Khandker Farid Uddin Ahmed
Professor
Department of Mathematics
BUET, Dhaka-1000
Member
4. 

Dr. Salma Parvin
Professor
Department of Mathematics
BUET, Dhaka-1000
Member
5. 

Dr. Md. Mustafa Kamal Chowdhury
Former Professor
Department of Mathematics
BUET, Dhaka-1000
Member
(External)

AUTHOR'S DECLARATION

I hereby announce that the work which is being presented in this thesis entitled

“NUMERICAL STUDY OF CONTROLLING BLOOD FLOW THROUGH A STENOSED ARTERY USING POWER-LAW FLUID”

submitted in partial fulfillment of the requirements for the declaration of the degree of Master of Science, Department of Mathematics, BUET, Dhaka, is an authentic record of my own work. The work is also original except where indicated by and attached with special reference in the context and no part of it has been submitted for any attempt to get other degrees or diplomas. I authorize Bangladesh University of Engineering and Technology to lend this thesis to other institutions or individuals for the purpose of scholarly research.



(MD. AMZAD HOSSAIN)

Date: 1st October, 2019

PERMIT OF RESEARCH

This is to endorse that the work presented in this thesis is carried out by the author under the supervision of Dr. Rehana Nasrin, Professor, Department of Mathematics, Bangladesh University of Engineering and Technology (BUET), Dhaka-1000, Bangladesh.



Dr. Rehana Nasrin
Professor
Dept. of Mathematics
BUET, Dhaka-1000



Md. Amzad Hossain

Dedicated to
My Parents & Teachers

ACKNOWLEDGEMENT

I would like to affirm the notable recognizance of Almighty's continual mercy, because no work would have been possible to accomplish the goal line without help of Allah. With great pleasure I take this opportunity to place on record her deepest respect and sincerest gratitude to my Supervisor Prof. Dr. Rehena Nasrin, Department of Mathematics, Bangladesh University of Engineering and Technology, Dhaka for her expert guidance and valuable suggestions throughout this work. It would not have been possible to carry out this study successfully without continuous inspiration, guidance, constant support, intuitive suggestions and relentless encouragement from supervisor.

I owe a favor to Dr. Md. Mustafizur Rahman, professor and Head, Department of Mathematics, Bangladesh University of Engineering and Technology, for his support in allowing me to use the departmental facilities in various stages of my work.

I am also deeply indebted to Prof. Dr. Khandker Farid Uddin Ahmed and Prof. Dr. Salma Parvin, Department of Mathematics, BUET for their wise and liberal cooperation in providing me all necessary help from the department during my course of M.Sc. Degree. I wish to thank all staff of the Department of Mathematics, Bangladesh University of Engineering and Technology, for their cooperation in this work.

I would like to take the opportunity to thank Dr. Md. Mustafa Kamal Chowdhury, Former Professor, Department of Mathematics, Bangladesh University of Engineering and Technology, BUET. I am grateful to him for his valuable suggestions to improve this thesis work.

Finally, I would like to express my gratitude to my dear mother and brothers for their steadfast love and support. They have kept me going through the most difficult times.

ABSTRACT

Blood flow in artery has vital aspects due to the engineering as well as the medical implicational point of view. A non-Newtonian model for blood flow for a stenosed artery in human blood vessel has been studied numerically in this research. The non-Newtonian power-law model of blood flow has been considered for numerical investigation. The governing system of equation based on incompressible Navier-Stokes equations with externally imposed magnetic resonance has been generalized to take into account blood properties. The objectives of this research are to investigate the effects of inlet velocity and imposed magnetic field on the blood flow through the artery. Finite element method of Galerkin's weighted residual has been employed to solve the governing system of equation with proper boundary conditions. The numerical simulation has been conducted for various inlet velocities from 0.005 to 0.1 m/s and magnetic field strength from 0 to 12 tesla with good convergence of the iterative scheme. Results have been shown in velocity, surface plot of velocity, pressure and viscosity contours. Cross-sectional plots of velocity magnitude, pressure and viscosity across the stenotic contraction have also been displayed graphically. Results from the blood flow simulations indicate that viscosity increases due to increasing values of inlet velocity of blood and magnetic strength.

TABLE OF CONTENTS

<u>Items</u>	<u>Page</u>
BOARD OF EXAMINERS	Error! Bookmark not defined.
AUTHOR'S DECLARATION	ii
PERMIT OF RESEARCH	Error! Bookmark not defined.
ACKNOWLEDGEMENT	vi
ABSTRACT	VII
TABLE OF CONTENTS	viii
NOMENCLATURE	X
LIST OF TABLE	xi
LIST OF FIGURES	xii
CHAPTER 1: INTRODUCTION	1
1.1 Introduction	1
1.2 Literature Review	1
1.3 Objectives	5
1.4 Outline of the Thesis	6
CHAPTER 2: PRELIMINARIES AND BACKGROUND	7
2.1 Introduction	7
2.2 Density of Blood	7
2.3 Hemodynamics	8
2.4 Non-Newtonian Fluid Flows	8
2.5 Power-Law Model	10
2.6 Magnetic Field	12
2.7 Cardiovascular System	14
2.8 Viscosity of Blood	15
2.9 Constitution of Blood	17
CHAPTER 3: NUMERICAL MODELING OF BLOOD FLOW	19
3.1 Introduction	19
3.2 Physical Model	19
3.3 Governing Equations	19
3.4 Solution Procedure	21
3.4.1 Mesh generation	21
3.4.2 Grid independent test	22
CHAPTER 4: RESULTS AND DISCUSSIONS	23

4.1 Introduction	23
4.2 Effect of Velocity	23
4.3 Effect of magnetic field	30
CHAPTER 5: CONCLUSION AND RECOMMENDATIONS	37
5.1 Conclusions	37
5.2 Recommendations	37
REFERENCES	39

NOMENCLATURE

B	Magnetic field intensity [tesla]
K	Consistency coefficient
m	Blood consistency coefficient
n	Blood flow behavior index
p	Blood flow pressure [Pa or $mmHg$]
u	Velocity components (along x direction) [m/s]
v	Velocity components (along y direction) [m/s]

Greek symbol

σ_{ij}	Shear stress (normal) [Pa]
$\gamma \square$	Shear rate [s^{-1}]
$\dot{\gamma}_{\text{.....}}$	Lower shear rate limit
τ_{ij}	Shear stress (tangential) [Pa]
τ_w	Wall shear stress [Pa]
μ	Fluid viscosity [Ns/m^2]
ρ	Blood density [kg/m^3]
σ	Electrical conductivity
λ	Curve fitting parameters

Abbreviation

HCT	= Hematocrite
BMI	= Body mass index
MRI	= Magnetic resonance imaging
WSS	= Wall shear stress
CFD	= Computational fluid dynamics
BMD	= Bone mineral density
SD	= Standard deviations
MHD	= Mulberry heart disease
RPM	= Remote patient monitoring
LOCD	= Lab-on-a-cd
LOC	= Lab-on-a-chip

LIST OF TABLE

Items	Table Caption	Page
Table 3.1	Grid test at $u_i = 0.01$ m/s, $B = 2$ tesla	22

LIST OF FIGURES

Items	Figure Caption	Page
Figure 2. 1	Types of time-independent non-Newtonian fluid	9
Figure 2.2	Power law model fits for two cosmetic emulsions	11
Figure 2.3	Cardiovascular system	14
Figure 2.4	Coronary-artery-disease-coronary-bypasses	15
Figure 2.5	Flow-pressure relationship of water and blood	16
Figure 2.6	Relative viscosity	17
Figure 2.7	Shape of a red cell	18
Figure 3.1	Schematic diagram of a stenosed artery	19
Figure 3.2	Finite element mesh of the computational domain	21
Figure 4.1	Velocity contour inside artery for various inlet blood velocity at $B = 2$ tesla	25
Figure 4.2	Surface plot of artery for various inlet blood velocity at $B = 2$ tesla	26
Figure 4.3	Pressure contour inside artery for various inlet blood velocity at $B = 2$ tesla	27
Figure 4.4	Viscosity contour of artery for various inlet velocity at $B = 2$ tesla	28
Figure 4.5	Cross-sectional plot of (a) velocity magnitude and (b) shear rate for inlet velocity variation across the stenotic contraction	29
Figure 4.6	Velocity contour inside artery for various magnetic field at $u = 0.01$ m/s	32
Figure 4.7	Surface plot of artery for various magnetic field at $u = 0.01$ m/s	33
Figure 4.8	Pressure contour inside artery for various magnetic field at $u = 0.01$ m/s	34
Figure 4.9	Viscosity contour of artery for various magnetic field at $u = 0.01$ m/s	35
Figure 4.10	Cross-sectional plot of (a) velocity magnitude and (b) shear rate for magnetic field variation across the stenotic contraction	36

CHAPTER 1: INTRODUCTION

1.1 Introduction

Blood is considered as a fundamental fluid with major importance in physiopathology that remains a factor of heart failure and other diseases. The information of blood obtained from this study can be useful in the development of diagnosis tools for many diseases. The analysis of magnetic field effect will be useful to control blood flow in diseased state. Blood flow problem through tapered arteries becomes difficult at some region because it has been observed through clinical and sub-clinical examinations that such a condition can lead to hemorrhage and local thrombosis. This research will help in efficient way of such blood flow system of cardiac patient.

1.2 Literature Review

Razavi *et al.* [1] studied the power-law model produces higher deviations, in terms of velocity and wall shear stress in comparison with other models while generalized power-law and modified-Casson models are more prone to Newtonian state. The authors observed that increasing stenosis intensity causes flow patterns more disturbed downstream of the stenosis and wall shear stress (WSS) appear to develop remarkably at the stenosis throat. Shah [2] studied the effect of non-Newtonian behavior of blood flow through a radially non-symmetric multiple stenosis artery using Herschel-Bulkely fluid model.

The non-Newtonian fluid is only remarkably important at low shear rates and also in small arteries and capillaries with strain rates lower than 100 s^{-1} . Akbar and Nadeem [3] found that the hemodynamics behavior of the blood flow is influenced by the presence of the arterial stenosis. The authors discussed Carreau fluid model for blood flow through a tapered artery with a stenosis. Sapna Singh and Shah [4] stated that power-law model is able to predict the main characteristics of the physiological flows and may have some interest in biomedical application. The authors found that the resistance to blood flow, wall shear stress and apparent viscosity increase as stenosis size and length increases but decreases as stenosis shape parameter increases. Due to physiological importance of body acceleration, many researchers

proposed blood flow with body acceleration. Tanwar *et al.* [5] considered MHD pulsatile flow of couple stress fluid through an inclined circular tube with periodic body acceleration. Singh *et al.* [6] performed disease manifested itself as a local degenerative process which hardens the vessel walls and narrowed their lumen. As such the flow of blood to various parts of the body has been restricted. The arterial wall deforms as a result of pulsatile pressure over each cardiac cycle and other mechanical loads. Steinman *et al.* [7] reported the deformation creates forces within the vascular wall, which when normalized by cross-sectional area are referred to as wall stresses.

The blood flow is characterized by the generalized power-law model. A finite difference scheme was employed to solve the governing equations numerically by Ismail *et al.* [8]. The authors showed the effect of pulsation, stenosis severity, Reynold's number and Womersley number on the flow blood behavior. Hasan and Das [9] studied numerical simulation of sinusoidal fluctuated pulsatile laminar flow through stenotic artery. Akbar [10] discussed the blood flow analysis using Prandtl fluid model in tapered stenosed arteries. The author observed that due to increase in Prandtl fluid parameters, the stenosis shape and maximum height of the stenosis the velocity profile decreases. Madadelahi and Shamloo [11] presented Newtonian and generalized Newtonian reacting flows in serpentine microchannels, pressure driven and centrifugal micro-fluidics. The authors used a comprehensive 3D numerical simulation of reacting flows in micro scale dimension through centrifugal, or Lab-On-a-CD (LOCD), and pressure-driven, or Lab-On-a-Chip (LOC) devices.

Uddin and Alim [12] investigated the significance of symmetry and non-symmetry stenosis effects of blood flow and quantify some of the most relevant non-Newtonian characteristics of blood flow in blood vessels. Their blood flow simulations indicated that non-Newtonian behavior has considerable effects on instantaneous flow patterns. Bali and Awasthi [13] performed a Casson fluid model for multiple stenosed artery in the presence of magnetic field. The authors showed the effect of magnetic field, height of stenosis, parameter determining the shape of the stenosis on velocity field, volumetric flow rate in stenotic region and wall shear stress at surface of stenosis. Rahman *et al.* [14] performed a comparative study of Newtonian and non-Newtonian blood flow through a stenosed carotid artery. The authors showed the results of Newtonian and non-Newtonian condition follow each other at peak systole. They also showed the results of Newtonian and non Newtonian condition may be same at the throat

region but different at the pre and post stenotic region. Naddem *et al.* [15] investigated blood flow through a tapered artery with a stenosis, assuming the flow was steady and blood was treated as non-Newtonian power-law fluid model. The authors found exact solution that had been evaluated for velocity, resistance impedance, wall shear stress and shearing stress at the stenosis throat. Long *et al.* [16] constructed three axisymmetrical and three asymmetrical stenosis models with area reduction of 25, 50 and 75%, respectively. The authors demonstrated that the formation and development of flow separation zones in the poststenotic region are very complex, especially in the flow deceleration phase.

Abdel Baieth [17] investigated apparent additive viscosity of animal blood after exposing to electromagnetic fields (EMFs). The author indicated that hematocrite (HCT) increased as EMF increases while the viscosity decreased with the increase of EMF. Peskin [18] extended the solution of the Navier-Stokes equations in the presence of moving immersed boundaries which interact with the fluid. The authors presented calculations with natural valve and with a prosthetic valve. Kumar and Diwakar [19] conducted a mathematical model of power-law fluid with an application of blood flow through an artery with stenosis. The authors showed the effect of stenosis on the cardiovascular system by studying the flow characteristics of blood in stenotic region in artery. Chandra and Singh [20] investigated the resistance to flow across mild stenosis situated symmetrically on steady blood flow through arteries with uniform or non-uniform cross section. The authors found an analytical solution for power-law fluid. Imaeda and Goodman [21] performed some aspects of the problem of computation of non-linear pulsatile blood flow in large arteries. The authors extended computational method to include effects of viscoelasticity of arterial walls.

Srivastava [22] investigated blood flow through a narrow catheterized artery with an axially nonsymmetrical stenosis. The author found that the impedance increased with the catheter size, the hematocrit and the stenosis size but decreased with the shape parameter. Ponalagusamy [23] developed an analysis which could be used to determine the more accurate values of the apparent viscosity of blood, agreeability, rigidity and deformability of red cells. Srivastava and Saxena [24] presented a brief review of the literature on artery catheterization with and without stenosis. A mathematical model for blood flow through stenosed arteries with axially variable peripheral layer thickness and variable slip at the wall has been considered by Thurstan [25]. The model in this article consisted of a core surrounded by a

peripheral layer. Sankar and Hemalatha [26] represented blood as a two-fluid model, consisting of a core region of suspension of all the erythrocytes assumed to be a Casson fluid and a peripheral layer of plasma as a Newtonian fluid. Chakravarty and Mandal [27] developed a two dimensional blood flow model through tapered arteries under stenotic conditions. The authors presented an improved shape of the time-variant overlapping stenosis in the tapered arterial lumen.

Leuprecht and Perktold [28] showed the computer simulation of non-newtonian effects on blood flows in large arteries. The authors demonstrated the viscoelastic behaviour of the local flow patterns in large arteries which was dependent on the shape of the flow domain. Srivastav and Agnihotri [29] studied non-Newtonian power-law blood fluid flow through bell-shaped stenosis artery. The authors presented blood flow to account for the non-Newtonian behavior by a power-law fluid. They expressed the flow characteristics, namely, the impedance, the wall shear stress, the shear stress at the stenosis throat that had been derived. They also presented some results concerning the dependence of these quantities on the geometrical parameters. Shahidian *et al.* [30] investigated flow analysis of non-Newtonian blood in a magneto hydrodynamic pump. The authors utilized a Power-law model for blood viscosity. They studied the velocity that increased by increasing the magnetic flux density and current. Halder [31] studied the effects of the shape of stenosis on the resistance to blood flow through an artery. The author conducted the resistances to flow decreases as the shape of stenosis changes and the maximum resistance that was attained in the case of symmetric stenosis. Mathur and Jain [32] developed a mathematical model for studying the non-Newtonian flow of blood through stenosed arterial segment. Tzirtzilakis [33] conducted a mathematical model of biomagnetic fluid dynamics (BFD) which was suitable for the description of the Newtonian blood flow under the action of an applied magnetic field. The model was consistent with the principles of ferrohydrodynamics and magnetohydrodynamics and was taken into account both magnetization and electrical conductivity of blood. Mandal [34] investigated an unsteady analysis of non-Newtonian blood flow through tapered arteries with a stenosis. The author studied the effects of the taper angle, wall deformation, and severity of the stenosis within its fixed length, steeper stenosis of the same severity, nonlinearity and non-Newtonian rheology of the flowing blood on the flow field.

Mantha *et al.* [35] investigated by performing computational fluid dynamic simulations of flow near 7 cerebral aneurysms using geometrical data obtained from clinical CT scans. The authors observed flow patterns that were found to occur in different types of aneurysms (bifurcation and sidewall), and can persist even after flow parameters are perturbed beyond the normal range of physiological flow conditions. Mekheimer and Kot [36] studied the micropolar fluid model for blood flow through a tapered artery with a stenosis. The authors founded the velocity profile, the wall shear stress distribution in the stenotic region and their magnitude at the maximum height of the stenosis that was discussed for different values of the parameters involved on the problem. Shukla *et al.* [37] investigated effects of stenosis on non-Newtonian flow of the blood in an artery. The authors showed that the resistance of flow and the wall shear increase with the size of the stenosis. Hershey *et al.* [38] investigated the temperature dependent of the power-law model in blood rheology.

1.3 Objectives

In view of the above literature, it is observed that the magnetic field effect for blood flow through arterial stenosis using Power-law fluid model has not been investigated yet. The numerical study focuses how to control blood flow in presence of magnetic field through stenotic artery using Power-law fluid model. In this research, how magnetic field controls blood flow through a tapered artery with a stenosis will be analyzed, assuming the flow is steady and blood is treated as non-Newtonian power-law fluid model.

The aim of this study is to investigate numerically the blood flow through a tapered artery with a stenosis, assuming the flow is steady and blood is treated as non-Newtonian power-law fluid model. However, the main objectives of the research are:

- i) To develop a 2D mathematical model for a stenosed arterial blood flow in presence of magnetic field.
- ii) To solve the mathematical model numerically.
- iii) To visualize blood flow through stenotic artery.
- iv) To investigate the effect of magnetic field on controlling velocity, pressure, viscosity and shear rate of blood flow through stenotic artery.

1.4 Outline of the Thesis

A brief description of the present numerical investigation of inlet velocity and magnetic field strength variation on blood flow through a stenosed artery have been presented in this thesis through five chapters as stated below:

The required literature review and importance of numerical study to understand the scope of this research has been provided in the Chapter 1.

Special emphasis on the principles of fluid dynamics and human circulatory system followed by the structure and function of arteries with mechanical property has been mentioned in Chapter 2. The cerebral/aortic stenosis represents one of the forms of cardiovascular diseases that to the aim and motivation of this research have also been discussed in this chapter.

The numerical modeling of blood flow has been highlighted in Chapter 3 and also in this chapter the numerical approach followed to solve the governing equations has been explained.

In Chapter 4, numerical results obtained from the present research have been represented with appropriate discussion.

Finally, in Chapter 5, the conclusions have been drawn and possible future research has also been mentioned.

CHAPTER 2: PRELIMINARIES AND BACKGROUND

2.1 Introduction

Computational Fluid Dynamics (CFD) modeling of hemodynamic blood flow requires some background in physiology, anatomy, pathology as well as principles of fluid dynamics before any modelling decisions are to be made. This chapter provides the required background to understand the scope of this research. The chapter begins with special emphasis on the principles of fluid dynamics and human circulatory system followed by the structure and function of arteries with mechanical property. The next section describes the human cardiovascular diseases and cerebral stenosis which represent one of the forms of cardiovascular diseases that lead to the aim and motivation of this research.

2.2 Density of Blood

This study tests the hypothesis that reduced blood flow to the lower extremities may affect bone remodeling, resulting in a decrease in bone mineral density (BMD). BMD was measured in the axial and appendicular skeleton of 1292 elderly women (mean age, 71 years) enrolled in the study of osteoporotic fractures. The ratio of the posterior tibial and brachial systolic blood pressures, the ankle/arm index, was used as a measure of blood flow to the legs. In the cross-sectional analysis, this index was positively correlated with BMD at the radius, calcaneus and hip, but not at the spine. A decrease in the index of 2 standard deviations (SD) (as might occur in patients with moderate arterial disease) was associated with a decrease of 3.7% in hip BMD. The effect size at the hip decreased from 3.7 to 1.8% (and was not statistically significant) when adjustment was made for smoking and/or body mass index (BMI). In the prospective analysis, the rate of bone loss at the hip and calcaneus was greater among women whose annual decrease in ankle/arm index was more than 1 SD greater than the mean decrease. This increase was independent of estrogen use, smoking, BMI, pattern of fat distribution, history of diabetes, exercise, and ability to walk. The results from this prospective community-based study provide the first evidence that among relatively healthy older women decreased vascular flow in the lower extremities may be associated with an increased rate of bone loss at the hip and calcaneus.

2.3 Hemodynamics

Hemodynamics or haemodynamics is the dynamics of blood flow. The circulatory system is controlled by homeostatic mechanisms, such as hydraulic circuits are controlled by control systems. Hemodynamic response continuously monitors and adjusts to conditions in the body and its environment. Thus hemodynamics explains the physical laws that govern the flow of blood in the blood vessels.

Blood flow ensures the transportation of nutrients, hormones, metabolic wastes, O₂ and CO₂ throughout the body to maintain cell-level metabolism, the regulation of the pH, osmotic pressure and temperature of the whole body, and the protection from microbial and mechanical harms.

Blood is a non-Newtonian fluid best studied using rheology rather than hydrodynamics. Blood vessels are not rigid tubes, so classic hydrodynamics and fluids mechanics based on the use of classical viscometers are not capable of explaining hemodynamics. The study of the blood flow is called hemodynamics. The study of the properties of the blood flow is called hemorheology.

2.4 Non-Newtonian Fluid Flows

A non-Newtonian fluid is a fluid whose flow properties differ in many ways from those of Newtonian fluids. Most commonly the viscosity of non-Newtonian fluids is not independent of shear rate or shear rate history. In practice, many fluid materials exhibits non-Newtonian fluid behaviour such as: salt solutions, molten, ketchup, custard, toothpaste, starch suspensions, paint, blood, and shampoo etc. In a Newtonian fluid, the relation between the shear stress and the shear rate is linear, passing through the origin, the constant of proportionality being the coefficient of viscosity

Among the three groups, the time independent non-Newtonian fluids are the most popular and easiest to handle in analysis. In this research, only this group of non-Newtonian fluids are considered. Figure 2.1 shows different types of time-independent non-Newtonian fluid.

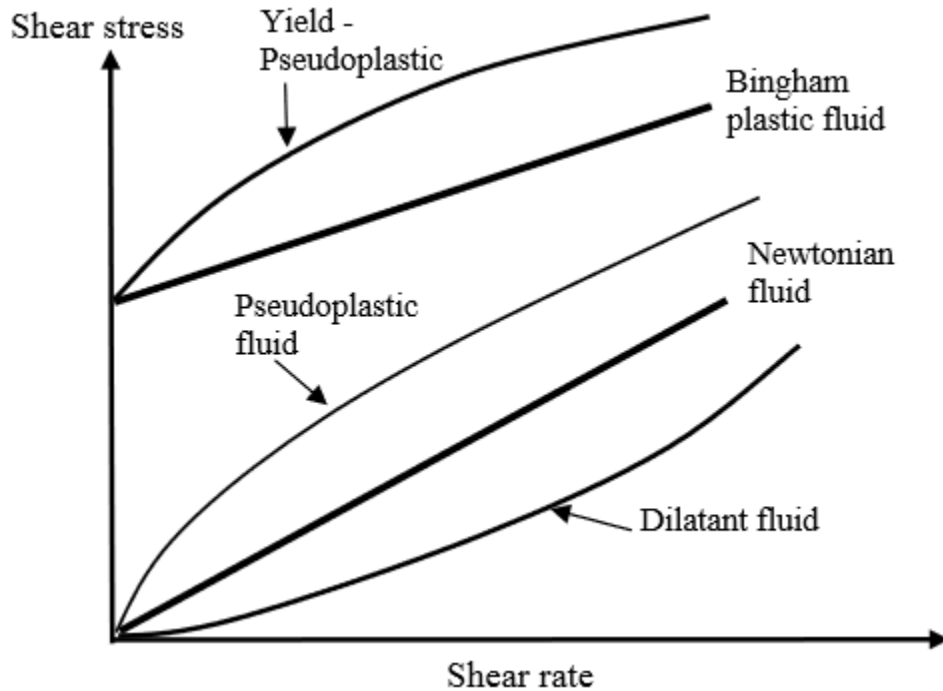


Figure 2. 1: Types of time-independent non-Newtonian fluid

The flow behaviour of this class of materials may be described by the following constitutive relation,

$$\tau_{yx} = f(\dot{\gamma}_{yx}) \quad (2.1)$$

This equation implies that the value of $\dot{\gamma}_{yx}$ and any point within the sheared fluid is determined only by the current value of shear stress at that point or vice versa. Depending upon the form of the function in equation (2.1), these fluids may be further subdivided into three types: shear-thinning or pseudoplastic, shear-thickening or dilatant and viscoplastic.

The relationship between shear stress and shear rate for this type of fluid can be mathematically expressed as equation (2.2):

$$\tau_{yx} = K(\dot{\gamma}_{yx})^n \quad (2.2)$$

So the apparent viscosity for the so-called power-law fluid is thus given by:

$$\mu = K(\dot{\gamma}_{yx})^{n-1} \quad (2.3)$$

For,

$n < 1$, the fluid exhibits shear-thinning properties

$n = 1$, the fluid shows Newtonian behavior

$n > 1$, the fluid shows shear-thickening behavior

In these equations, K and n are two empirical curve-fitting parameters and are known as the fluid consistency coefficient and the flow behaviour index, respectively. For a shear thinning fluid, the index may have any value between 0 and 1. The smaller the value of n , the greater is the degree of shear-thinning. For a shear-thickening fluid, the index n will be greater than unity. When $n = 1$, equations (2.3) becomes the constitutive equation of Newtonian fluid.

When there are significant deviations from the power-law model at very high and very low shear rates, it is necessary to use a model which takes account of the limiting values of viscosities ϵ_0 and ϵ_∞ . Based on the molecular network considerations, Carreau model [3] put forward the following viscosity model:

$$\frac{U - U_\infty}{U_0 - U_\infty} = \left[1 + (\lambda Y_{yx})^2 \right]^{(n-1)/2} \quad (2.4)$$

Where $n (< 1)$ and λ are two curve-fitting parameters. This model can describe shear thinning behavior over wide ranges of shear rates but only at the expense of the added complexity of four parameters. This model predicts Newtonian fluid behavior $\mu = \mu_0$ when either $n = 1$ or $\lambda = 0$ or both.

2.5 Power-Law Model

The power-law model is an easy-to-use model that is ideal for shear-thinning, relatively mobile fluids such as weak gels and low-viscosity dispersions. The model is nothing more than the Newtonian model, with an added exponent on the shear rate term:

$$\eta = KY^{n-1}$$

Here η = viscosity and Y = shear rate, K is often known as the consistency coefficient. This describes the overall range of viscosities across the part of the flow curve that is being modelled. Also, if the Power-law region includes 1s^{-1} shear rate then K is the viscosity or

stress at that point. The exponent n is known as the flow behavior index (or sometimes the rate index). For a shear thinning fluid: $0 < n < 1$. The more shear-thinning in the product and the closer n is to zero. Examples of Power-law model fits on viscosity/shear rate profiles of two cosmetic emulsions are shown in the figure 2.2.

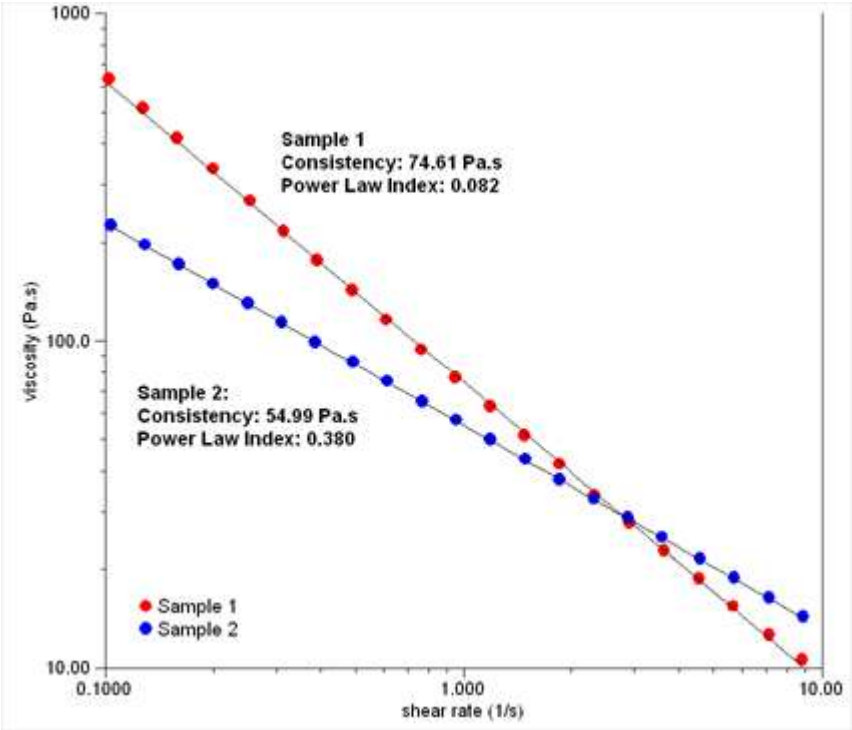


Figure 2.2: Power law model fits for two cosmetic emulsions

The power-law model describes the shear thinning effect of the drilling fluid. This model has two parameters to describe the behaviour of the fluid. As shown in Figure 2.2 the shear stress-shear rate relationship of the fluid passes through the origin with a power-law shape describes the behaviour of a power-law fluid.

$$\tau = K * Y^n$$

However, the power-law model for the low shear rate section still passes through the origin and does not explain the thixo-tropic properties of the drilling fluid. In the drill string where

high shear rate flow prevails, 600 RPM and 300 RPM data are applied to determine the flow parameters.

$$n_t = 3.32 \times \text{Log}\left(\frac{R_{600}}{R_{300}}\right)$$

$$K_t = \frac{R_{600}}{1022^{n_t}} = \frac{R_{300}}{511^{n_t}}$$

In the annulus, where low shear rate flow prevails, 100 RPM and 3 RPM data are applied to determine the flow parameters.

$$n_l = 0.657 \times \text{Log}\left(\frac{R_{100}}{R_3}\right)$$

$$K_l = \frac{R_{100}}{107.3^{n_l}} = \frac{R_3}{5.11^{n_l}}$$

Where

K = Consistency index, $\text{lb}\cdot\text{s}^n/100 \text{ ft}^2$

n = Flow behavior index

In the theory when flow behavior index exponent, n is equal to one, the power-law model reduces to the Newtonian fluid model and consistency index, K , has the unit of viscosity. If K is expressed in $\text{lb}_f\cdot\text{s}^n/100 \text{ ft}^2$ when n is equal to 1, the unit of K reduces to $\text{lb}_f\cdot\text{s}^n/100 \text{ ft}^2$.

2.6 Magnetic Field

Since blood consists of a suspension of red blood cells containing hemoglobin which contains iron oxide, it is quite apparent that blood is electrically conducting and exhibits magneto hydrodynamic flow characteristics.

The magnetic effect, the researchers say, all comes down to hemoglobin, the iron-based protein inside red blood cells. In the same way that iron filings align themselves along the field lines around a bar magnet, so the red blood cells align themselves along the straight field lines of Tao and Huang's electromagnet. This reduces viscosity in several ways. For one, the cells become streamlined with the direction of flow. The alignment also encourages the cells to stick together, forming clumps of various sizes. Although one might think clumps would increase viscosity, they actually have a lower total surface area compared with single cells,

and this cuts down on friction. What's more, the mixture of clump sizes allows more cells to pack into the same volume, with small cells fitting around the big clumps and allowing more room for movement.

One catch with the technique is that the blood flow must be in the same direction as the magnetic field. The effect wouldn't be the same when an entire body is in a magnetic resonance imaging (MRI) machine, for example, because blood vessels travel in all different directions.

Many authors have investigated the flow of blood through arteries in the presence of magnetic field under different conditions. In fact, the Lorentz force arising out of the flow across the magnetic lines of force acts on the constituent particles of blood and alters the hemodynamic indicators of blood flow. The potential use of such MHD principles in prevention and rational therapy of arterial hypertension shows that for steady flow of blood in an artery of circular cross-section, a uniform transverse magnetic field alters the flow rate of blood.

The biggest and most important component in an MRI system is the magnet. The magnet in an MRI system is rated using a unit of measure known as a Tesla. Another unit of measure commonly used with magnets is the gauss (1 Tesla = 10,000 gauss). The magnets in use today in MRI are in the 0.5-Tesla to 3.0-Tesla range, or 5,000 to 30,000 gauss. Extremely powerful magnets up to 60 Tesla are used in research [41]. Compared with the Earth's 0.5-gauss magnetic field, you can see how incredibly powerful these magnets are.

Because of the power of these magnets, the MRI suite can be a very dangerous place if strict precautions are not observed. Metal objects can become dangerous projectiles if they are taken into the scan room. For example, paperclips, pens, keys, scissors, hemostats, stethoscopes and any other small objects can be pulled out of pockets and off the body without warning, at which point they fly toward the opening of the magnet (where the patient is placed) at very high speeds, posing a threat to everyone in the room. Credit cards, bank cards and anything else with magnetic encoding will be erased by most MRI systems.

2.7 Cardiovascular System

The primary function of the heart and blood vessels is to transport oxygen, nutrients, and by products of metabolism. Oxygenated and nutrient rich blood is distributed to tissues via the arterial system, which branches into smaller and smaller blood vessels from arteries to arterioles to capillaries (where most exchange occurs). Deoxygenated blood and metabolic are returned from capillaries via venules and then vein. The heart functions as a pump to maintain circulation. The heart is a discrete organ, which in humans has four distinct chambers. Conceptually, there is the right side of the heart (right atrium and right ventricle) which receive blood returning from the periphery and send it to the lungs (via the pulmonary artery) for re-oxygenation. Once blood is re-oxygenated in the lungs it is returned to the left side of the heart via the pulmonary veins. After entering the left atrium, blood enters the left ventricle and is pumped into the aortic arch for distribution to the entire body. Figure 2.3 shows the schematic diagram of cardiovascular system.

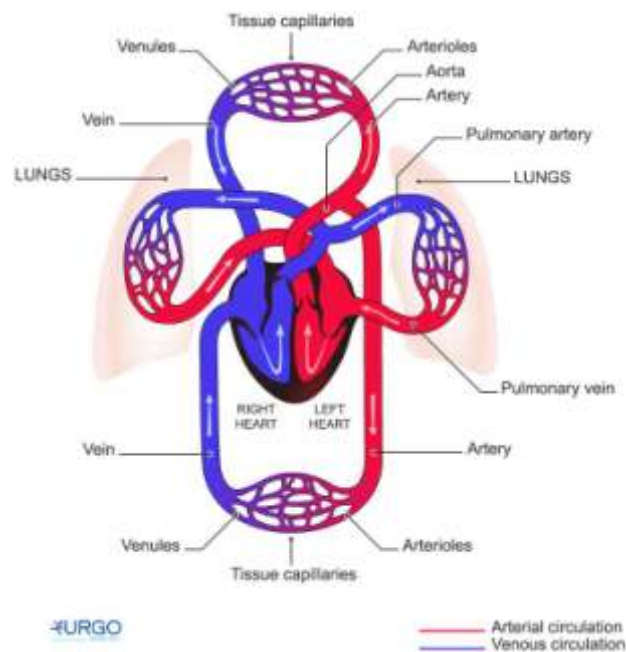


Figure 2.3: Cardiovascular system

Note also the heart is just like any other tissue in that it needs a continuous supply of oxygen and nutrients. The receives its blood supply from coronary arteries, which arise from the root of the aorta. The right and left coronary, coronary-artery-disease-coronary-bypass are show in the Figure 2.4.

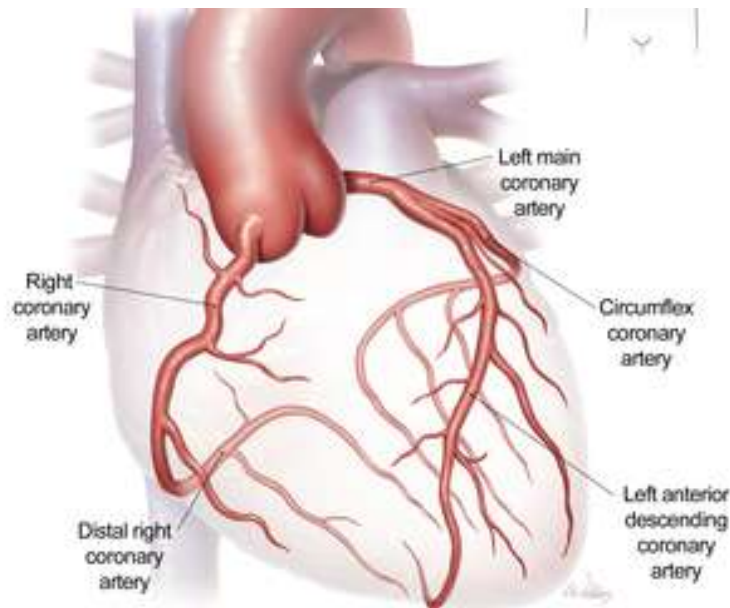


Figure 2.4: Coronary-artery-disease-coronary-bypass

2.8 Viscosity of Blood

Viscosity is an intrinsic property of fluid related to the internal friction of adjacent fluid layers sliding past one another (see laminar flow). This internal friction contributes to the resistance to flow as described by Poiseuille's equation. The interactions between fluid layers depend on the chemical nature of the fluid, and whether it is homogeneous or heterogeneous in composition. For example, water is a homogeneous fluid and its viscosity is determined by molecular interactions between water molecules. Water behaves as a Newtonian fluid and therefore under non-turbulent conditions, its viscosity is independent of flow velocity (i.e., viscosity does not change with changes in velocity). This is shown in the figure as a linear dashed line for the flow-pressure relationship of water. There is an inverse relationship between flow and viscosity; therefore, the greater the viscosity the smaller the slope of the

flow-pressure relationship, meaning that at a given driving pressure flow will be reduced at higher viscosities. Whole blood has a much higher viscosity than water and therefore the slope of the flow-pressure relationship is less steep. Unlike water, blood is non-Newtonian because its viscosity increases at low flow velocities (e.g., during circulatory shock). Low flow states permit increased molecular interactions to occur between red cells and between plasma proteins and red cells. This can cause red cells to stick together and form chains of several cells (rouleau formation) within the microcirculation, which increases the blood viscosity. Because of the high degree of interaction between the elements of blood when it is not flowing, a driving pressure significantly greater than zero is required for stationary blood to start flowing again. This is referred to as the yield stress required to initiate flow. Flow-pressure relationship of water and blood has been shown in the Figure 2.5.

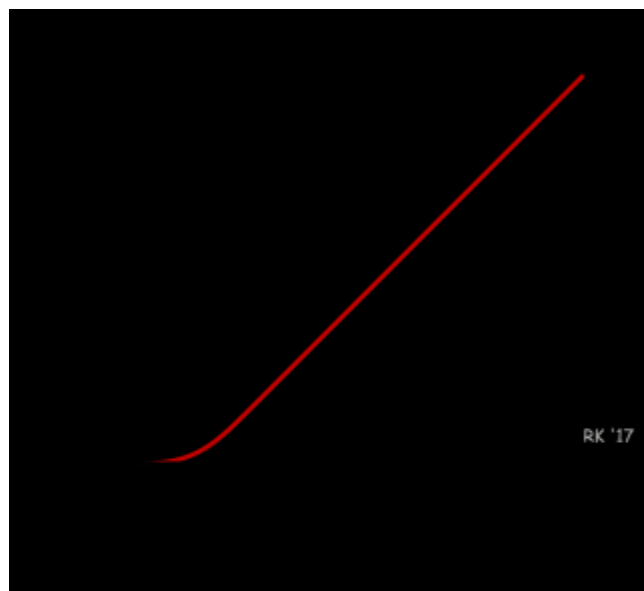


Figure 2.5: Flow-pressure relationship of water and blood

The addition of formed elements to plasma (red cells, white cells, and platelets) further increases the viscosity. Increasing red cell hematocrit increases relative viscosity. Note that: the increase is non-linear; increased hematocrit causes a disproportionate increase in relative viscosity. Therefore, blood viscosity strongly depends on hematocrit. At a normal hematocrit of 40%, the relative viscosity of blood is about 4. Patients with an abnormal elevation in red

cell hematocrit (polycythemia) have much higher blood viscosities. In fact, increasing the hematocrit from 40 to 60% (a 50% increase) increases the relative viscosity from 4 to 8 (a 100% increase). Increased viscosity increases the resistance to blood flow and thereby increases the work of the heart and impairs organ perfusion. Some patients with anemia have low hematocrits, and therefore reduced blood viscosities. Figure 2.6 shows the relative viscosity of blood.

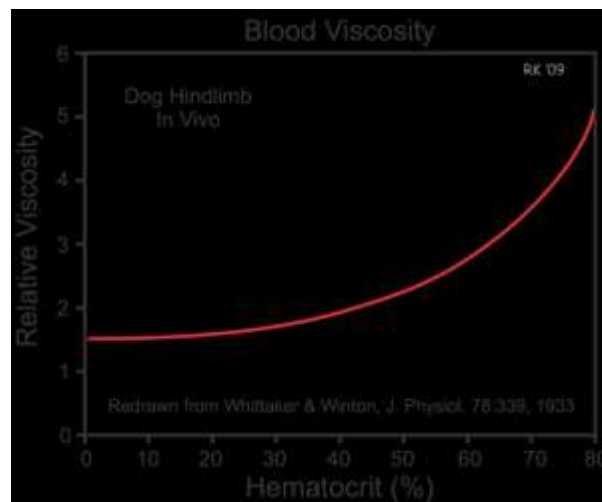


Figure 2.6: Relative viscosity of blood

2.9 Constitution of Blood

Blood is a body fluid in humans and other animals that delivers necessary substances such as nutrients and oxygen to the cells and transports metabolic waste products away from those same cells. Blood consists of a suspension of cells in an aqueous solution called plasma which is composed of about 90 percent water and 7 percent protein. There are about 5×10^9 cells in a milliliter (1cc) of healthy human blood, of which about 95 percent are red cells or erythrocytes whose main function is to transport oxygen from the lungs to all the cells of the body and the removal of carbon-dioxide formed by metabolic processes in the body to the lungs. About 45 percent of the blood volume in an average man is occupied by red cells. This fraction is known as the hematocrit. Of the remaining, white cells or leucocytes constitute about 1 percent of the total, and these play a role in the resistance of the body to infection. Platelets form 5 percent of the total, and they perform a function related to blood clotting.

In 5 liters of blood in the human body, there are about 25×10^{12} red cells. The mean life of a red cell is about 120 days and the total number of red cells which die per second is

$$\frac{25 \times 10^{12}}{120 \times 24 \times 60 \times 60} = 2.4 \times 10^6$$

The total number of red cells which serve a man in his lifetime of 60-70 years (about 200 cycles of 120 days each) is about 5×10^{15} . Their total volume is about $2.25 \times 200 = 450$ liters, so that in a lifetime about 0.5 ton of red blood cells are manufactured in our body. These cells supply oxygen to about 60 million cells of our body. It is noted that number of red cells in 1 cc of blood is more than the number of living human beings on the planet earth.

By considering the fact that 25×10^{12} cells occupy about $0.45 \times 5 = 2.25$ liters of blood, the mean volume of a red cell can be obtained as

$$\frac{2250}{2.5 \times 10^{11}} = 9 \times 10^{-11} \text{cc} = 9 \times 10^{-17} \text{m}^3 = 90 \text{m}^3$$

The volume of a red cell can also be obtained by considering the shape of a red cell which is a biconcave disc with an average diameter of about $8 \mu\text{m}$ and thickness varying from $1 \mu\text{m}$ at the center to about $2.2 \mu\text{m}$ at the ends. The shape of a red cell has been depicted in the Figure 2.7.

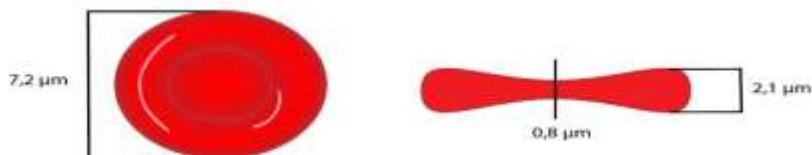


Figure 2.7: Shape of a red cell

CHAPTER 3: NUMERICAL MODELING OF BLOOD FLOW

3.1 Introduction

The blood circulation system, there are some strong hemodynamical features that can change in the rheological properties of blood and its components. It plays a major role in the development and progression of atherosclerotic plaques and other arterial lesions. In any physiological and pathological situations, the numerical study is an important tool for the interpretation and analysis of the circulatory system and can capture the rheological response of blood over a range of physiological flow conditions accurately.

3.2 Physical Model

In this research, the blood is assumed to be laminar, incompressible, and non-Newtonian. The physical model has been shown in the Figure 3.1, along with the important geometric parameters. The stenosed vessel is assumed to be two-dimensional with diameter 0.0062 m and length 0.031 m which reduces smoothly to one half in the stenosed region. Various velocity (m/s) is prescribed at the inlet and pressure is fixed to a constant at outlet. On the walls, no-slip conditions are used for velocity and homogeneous Neumann condition for the pressure. For Power-law fluid model is considered for dynamic viscosity. The stenosis cross-sectional area ration is 2:1 and thus a significant local acceleration of the flow is expected. A two dimensional arterial segment with arterial stenosis is considered with appropriate boundary conditions. The domain is permeated by the uniform external magnetic field B along x axis.

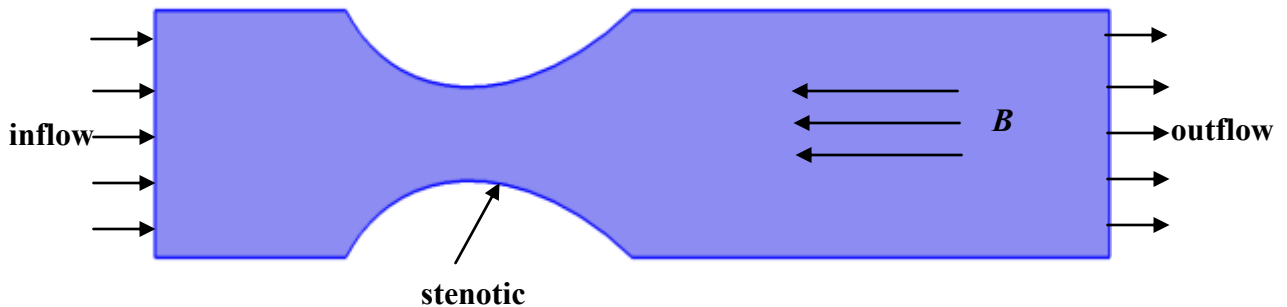


Figure 3.1: Schematic diagram of a stenosed artery

3.3 Governing Equations

The 2D numerical simulation has been performed in steady state conditions. The governing partial differential equations for non-Newtonian blood flow can be expressed as:

Continuity Equation:

$$\rho \left(\frac{\partial u}{\partial x} + \frac{\partial v}{\partial y} \right) = 0$$

X -Momentum Equation:

$$\rho \left(u \frac{\partial u}{\partial x} + v \frac{\partial u}{\partial y} \right) = -\frac{\partial p}{\partial x} + \mu \left(\frac{\partial^2 u}{\partial x^2} + \frac{\partial^2 u}{\partial y^2} \right)$$

Y-Momentum Equation:

$$\rho \left(u \frac{\partial v}{\partial x} + v \frac{\partial v}{\partial y} \right) = -\frac{\partial p}{\partial y} + \mu \left(\frac{\partial^2 v}{\partial x^2} + \frac{\partial^2 v}{\partial y^2} \right) - \sigma B^2 v$$

According to the power-law fluid model of Abdel Baieth [17], the viscosity is given by :

$$\mu = m \left(\dot{\gamma} \right)^{n-1}$$

$$\text{Here } \dot{\gamma} = \sqrt{\frac{1}{2} \left(\mathbf{u} + (\nabla \mathbf{u})^T \right)^2}$$

blood consistency coefficient $m = 0.01625 \text{ kg/ms}$,

blood flow behavior index $n = 0.71775$,

lower shear rate limit $\dot{\gamma}_{\text{lim}} = 0.1 \text{ 1/s}$,

the electrical conductivity $\sigma = 1.09 \text{ 1/}\Omega\text{s}$,

B is magnetic field intensity acting along x axis,

density of blood $\rho = 1060 \text{ kg/m}^3$.

The boundary conditions imposed on the blood flow have been written as follows:

On the inlet: velocity $u = u_i$ m/s, $v = 0$ m/s,

On the outlet: no viscous stress, pressure $p = 0$ Pa,

On the other boundaries: no slip condition $u = v = 0$ m/s.

3.4 Solution Procedure

By using the Galerkin weighted residual finite element technique ([39], [40]) the continuity and momentum equations have been solved. In this method, the solution domain has been discretized into finite element meshes, which have been composed of non-uniform triangular elements. Then the nonlinear governing partial differential equations have been transferred into a system of integral equations by applying Galerkin weighted residual method. The basic unknowns for the governing partial differential equations are the velocity components u , v and the pressure P . The six nodes with triangular element have been used in this numerical research. All six nodes have been associated with velocities as well as temperature while three corner nodes with pressure. The nonlinear algebraic equations so obtained have been modified by imposition of boundary conditions. These modified nonlinear equations have been transferred into linear algebraic equations by using Newton's method. Finally, these linear equations have been solved by using triangular factorization method. The convergence criterion for the solution procedure has been defined as $|\psi^{n+1} - \psi^n| \leq 10^{-6}$, where n is the number of iteration and is a function of u , v and p .

3.4.1 Mesh generation

Meshing the complicated geometry make the finite element method a powerful technique to solve boundary value problems occurring in a range of engineering applications. Figure 3.2 shows the mesh configuration of present physical domain with triangular finite elements.

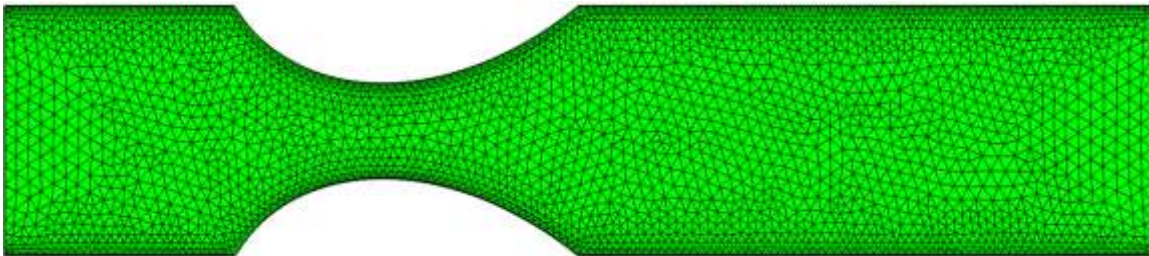


Figure 3. 2: Finite element mesh of the computational domain

3.4.2 Grid independent test

To facilitate the proper grid size for this study, a grid independence test is conducted with five types of mesh for through an rectangular enclosure. In the present work, five different non-uniform grid systems with the following number of elements within the resolution field: 5216, 9217, 22692, 54974 and 101272 have been examined. Table 3.1 shows the shear rate on the grid size. The scale of the shear rate for 54974 elements shows a little difference with the results obtained for the other elements. Hence, considering the non-uniform grid system of 54974 elements is preferred for the computation. Since, it is noticed that no further improvement is found for higher values.

Table 3.1: Grid test at $ui = 0.01$ m/s, $B = 2$ tesla

Nodes (elements)	9234 (5216)	15732 (9217)	37758 (22692)	89631 (54974)	159144 (101272)
Shear rate (1/s)	4.6163	5.0187	5.3252	5.6676	5.668
Time [s]	59	122	323	475	789

CHAPTER 4: RESULTS AND DISCUSSIONS

4.1 Introduction

Present numerical research deals with the blood flow through a stenosed human artery for different values of inlet blood velocity from 0.005 to 0.1 m/s and magnetic field strength from 0 to 12 tesla. The results have been shown in terms of velocity, plot of velocity magnitude, pressure distribution and viscosity contours. Also the cross sectional plots of velocity, pressure and viscosity magnitudes at the stenosed position of artery for the effect of magnetic field have been presented graphically.

4.2 Effect of Velocity

Figure 4.1 shows the velocity contour for stenosed artery with $B = 2T$. It is seen that, higher velocity exist at the central area of the artery whereas the lower velocity is at the wall because of no slip condition. The velocity contours are parallel at lowest inflow velocity of blood 0.005 m/s. A vortex creates near the upper wall for $u_i = 0.01$ m/s. This vortex increases in size for further increment of blood velocity. Finally, two big vortexes create near top and bottom surface if the artery for highest velocity 0.1 m/s.

The surface plot of the velocity magnitude has been shown in the Figure 4.2. The flow field takes the shape of the artery that is from the inlet it converges to the stenosed area and from there it diverges to the outlet. Due to increasing inlet blood velocity, the mid part of the artery has higher magnitude and the area of this mid part becomes larger in the surface plot.

As shown in the Figure 4.3, pressure lines are parabolic shape at the inlet and outlet port and on the other area; they are almost parallel to the vertical line. The pressure distribution becomes maximum near the inlet and stenosed portion of the artery. For all three cases, pressure becomes lower with the length of the artery while after the stenosis it becomes very low indicates lower velocity at that region.

Figure 4.4 displays the viscosity contour for the considered inlet blood velocity variation. Viscosity has the similar pattern as the velocity. That is higher viscosity exists at the central area of the artery whereas the lower values are at the wall because of no slip condition.

Maximum viscosity exists at the middle part of the stenosis due to the contraction of the domain.

Figure 4.5(a-b) depicts the cross sectional plot of velocity magnitudes and shear rate versus arc length at the middle of the stenosed part, respectively. The velocity profile is not exactly parabolic, slightly distorted. From this figure it is clearly seen that, velocity magnitude at the cross sectional line is about 1 m/s at inlet velocity 0.005 m/s and 2 m/s for inlet velocity 0.1 m/s due to the stenosis. Shear rates across the stenotic contraction for lower velocity upto 0.01 m/s are almost linear pattern but for other inlet velocity it is parabolic shape.

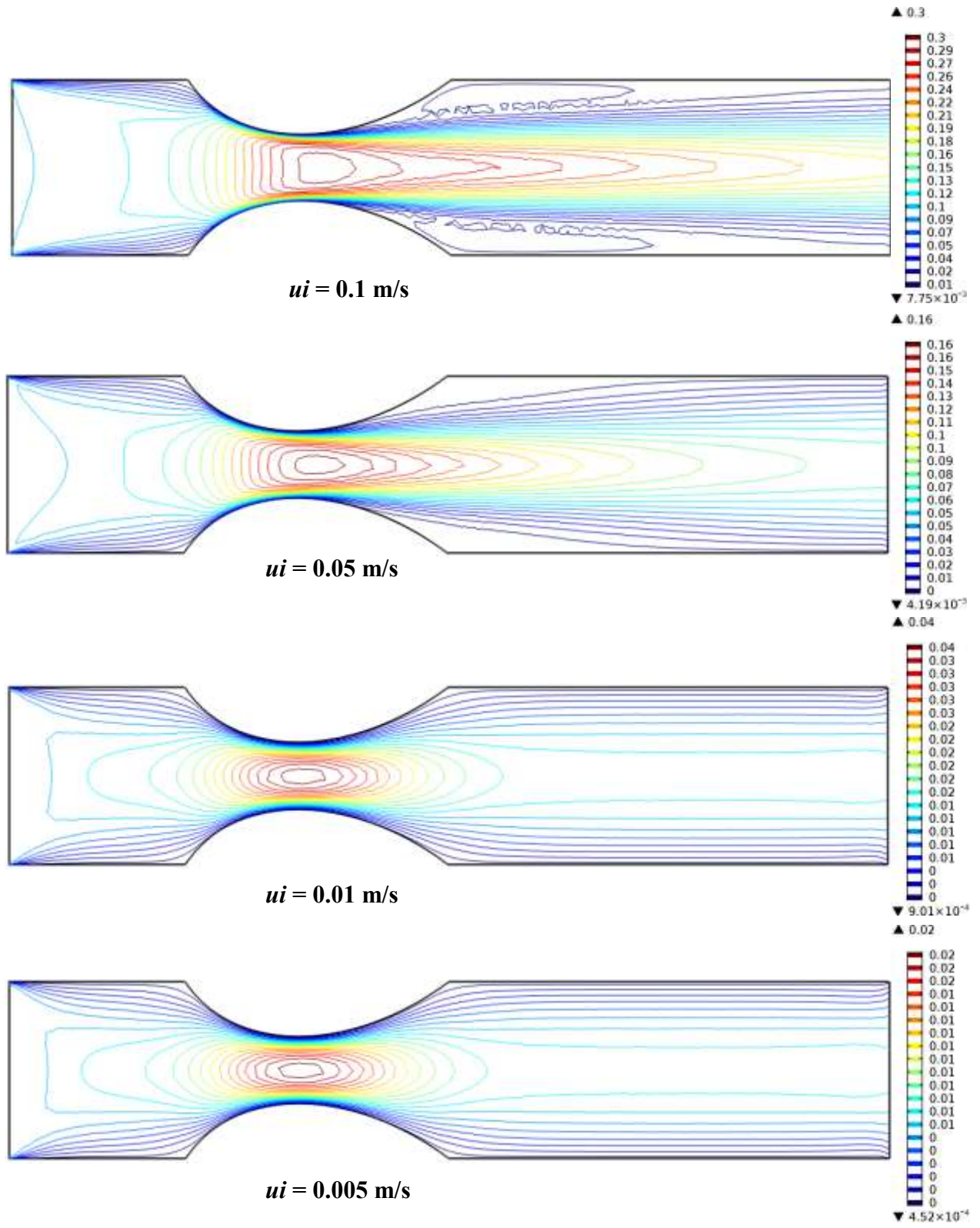


Figure 4.1: Velocity contour inside artery for various inlet blood velocity at $B = 2$ tesla

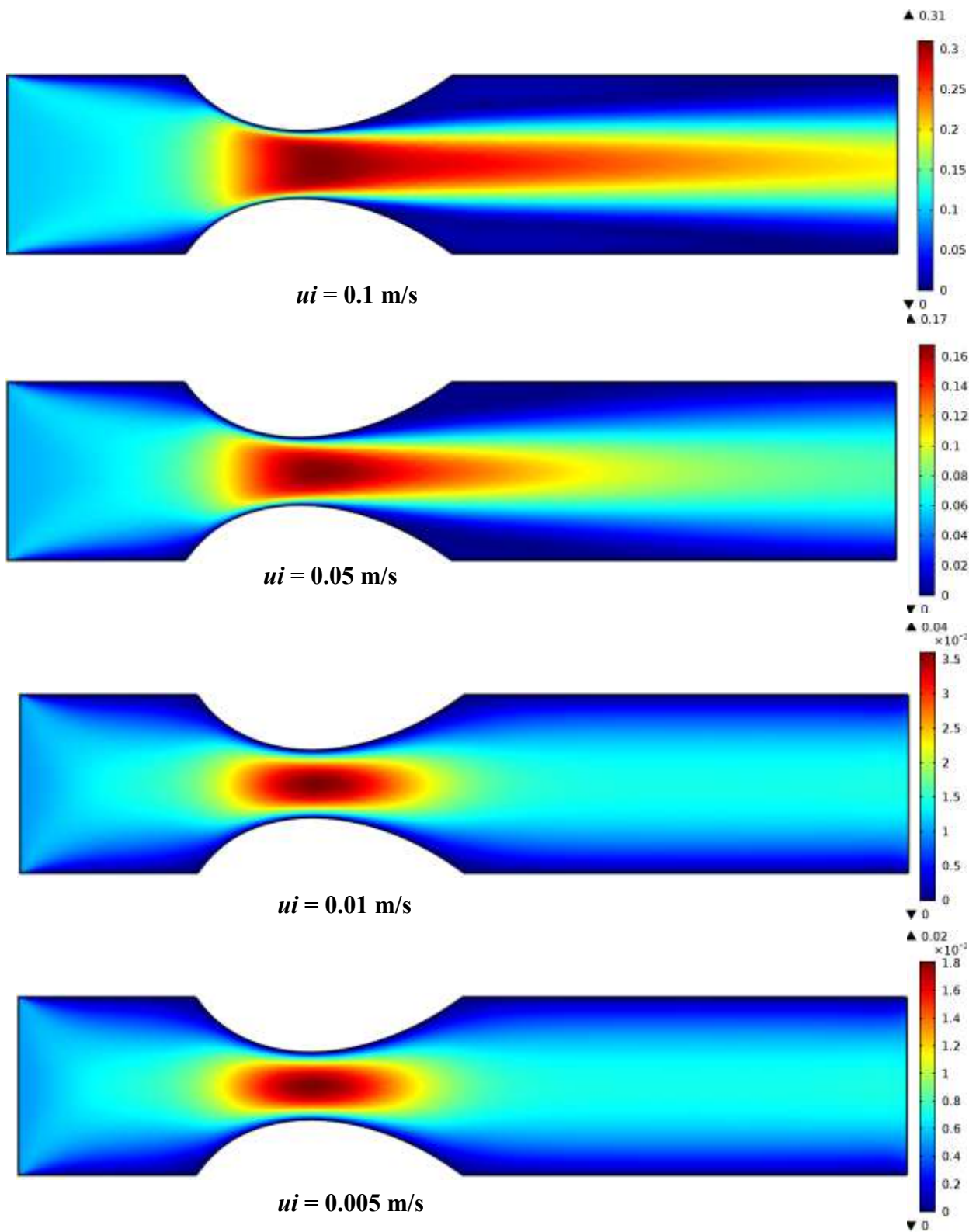


Figure 4.2: Surface plot of velocity magnitude artery for various inlet blood velocity at $B = 2$ tesla

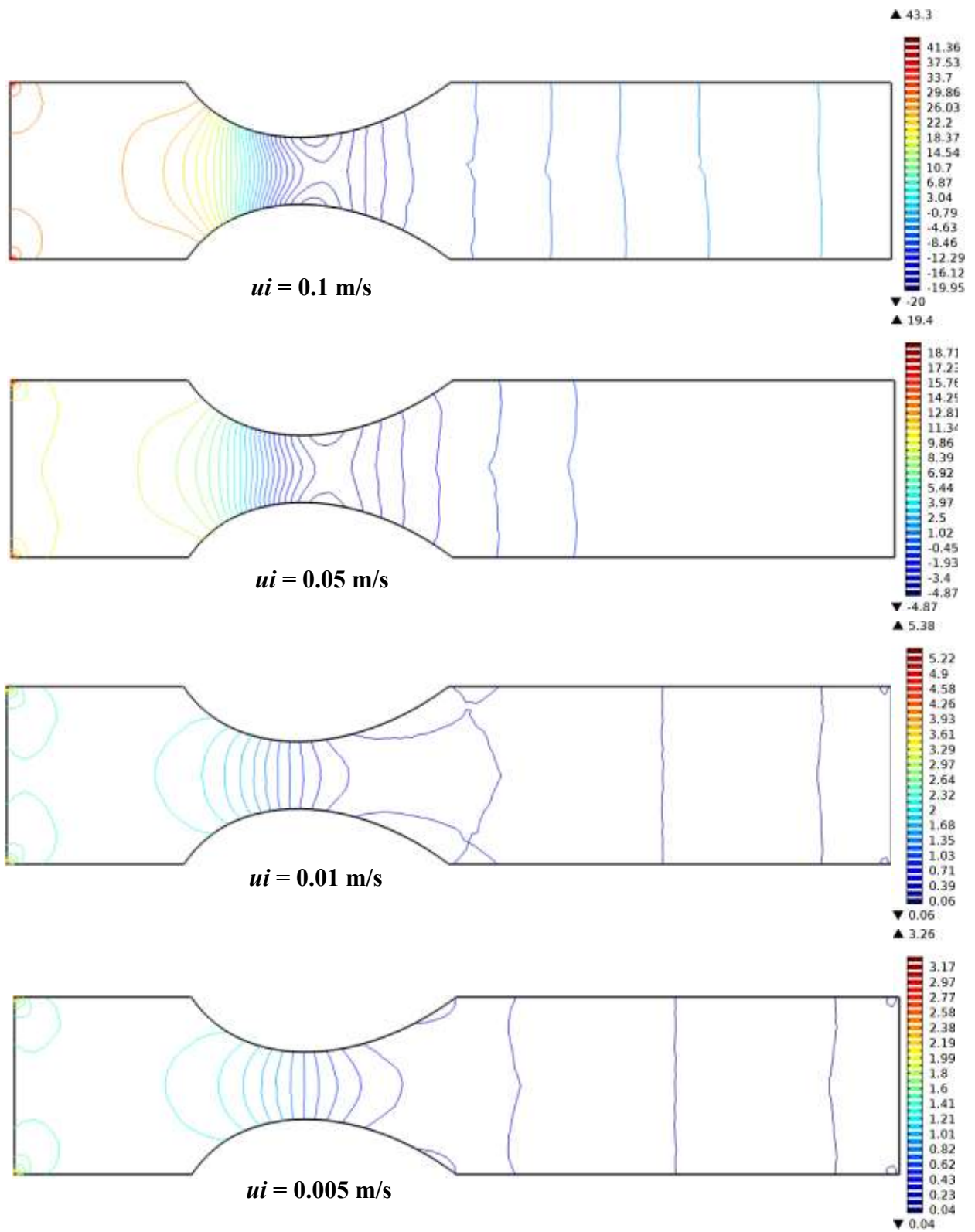


Figure 4.3: Pressure contour inside artery for various inlet blood velocity at $B = 2$ tesla

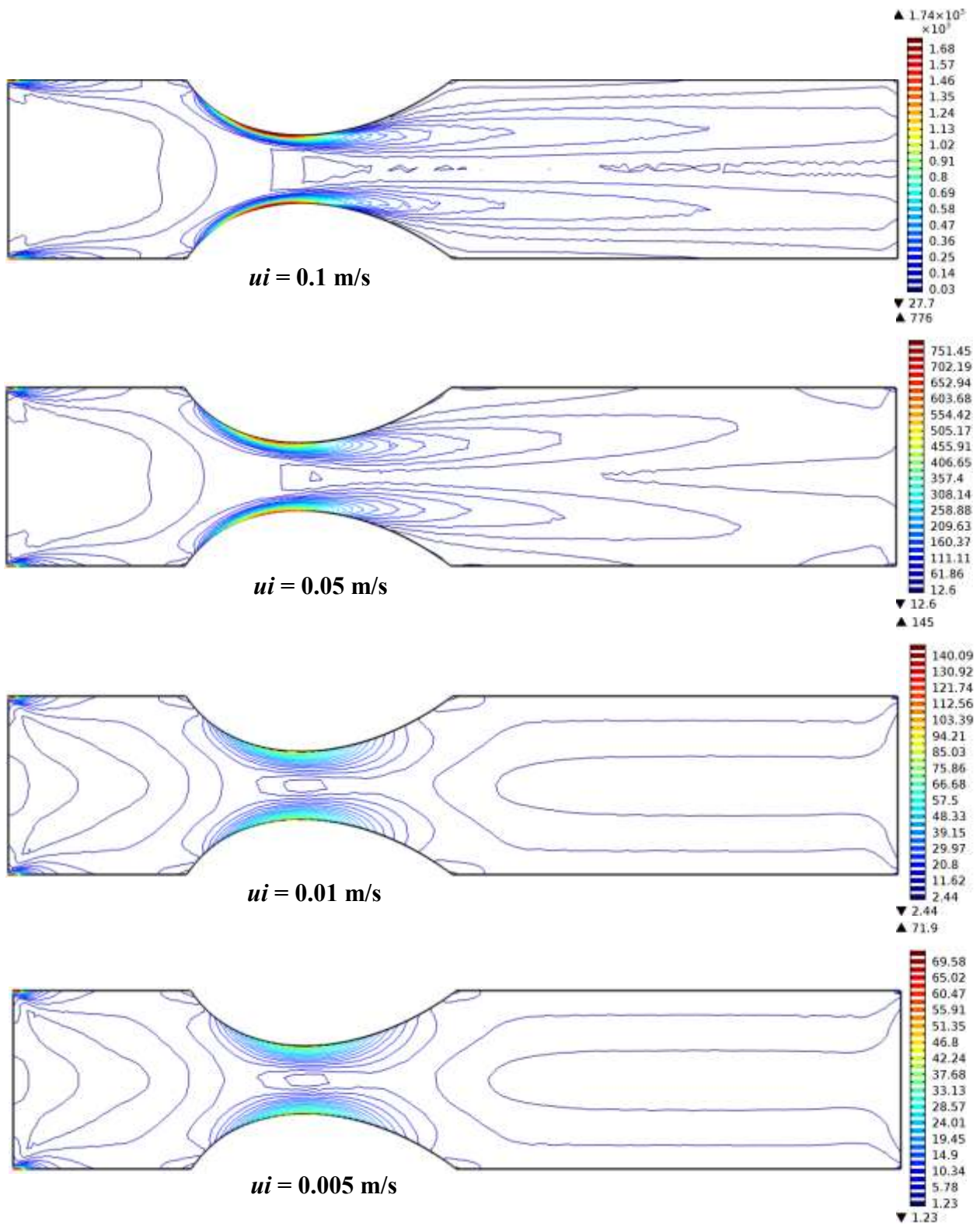
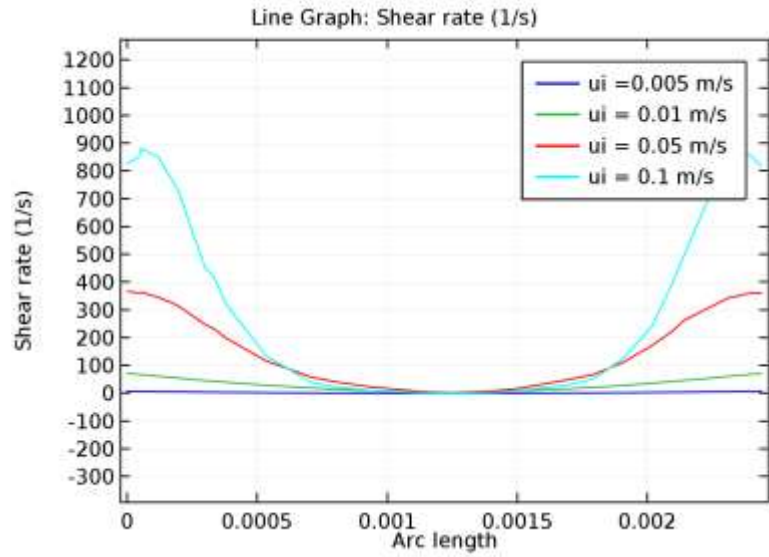
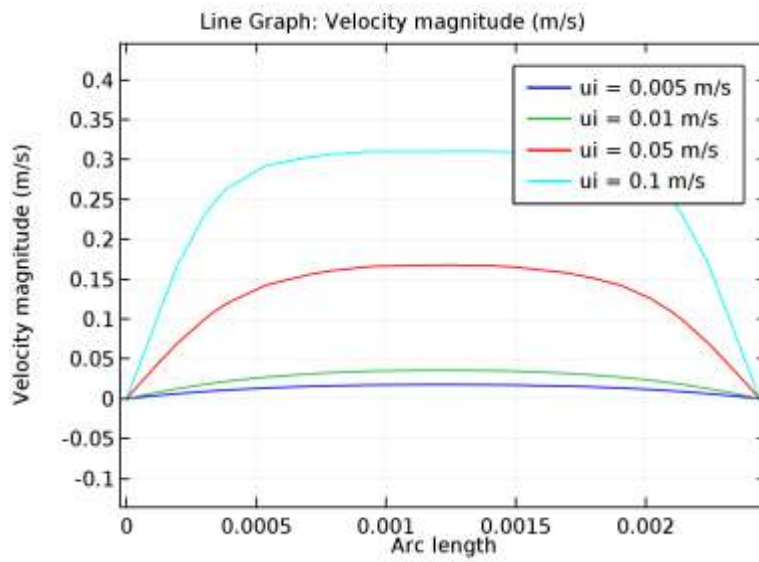


Figure 4.4: Viscosity contour of artery for various inlet blood velocity at $B = 2$ tesla



(b)



(a)

Figure 4.5: Cross-sectional plot of (a) velocity magnitude and (b) shear rate for inlet velocity variation across the stenotic contraction

4.3 Effect of magnetic field

Figure 4.6 shows the velocity contour for the effect of magnetic strength (from 0 to 12 tesla) inside the stenosed artery with fixed inlet blood velocity $u = 0.01$ m/s. It is seen that, higher velocity exists at the central area of the artery whereas the lower velocity is at the wall because of no slip condition. The velocity contours at the inlet portion are of rectangular shape and at the stenosed portion it becomes elliptical. Maximum velocity contours exist at the middle part of the stenosis. The direction of the flow field takes the parallel shape at the outlet portion so that from the inlet it converges to the stenosed area and from there it diverges to the outlet. There is no significant change of velocity contours due to the change of magnetic field strength.

The surface plot of the velocity magnitude has been shown in the Figure 4.7. Here the changing color from blue to red represents lower to higher magnitude for all cases. The flow field converges to the stenosed area and diverges from there to outlet. Due to increasing magnetic field strength, the mid part of the artery has higher magnitude and the area of this mid part becomes larger in the surface plot.

Figure 4.8. shows the pressure distribution when the magnetic field strength changes. The pressure lines at the inlet are almost parallel to the vertical wall and become parabolic at the stenosed portion. The maximum number of pressure line is in the stenosed portion of the artery. After the stenosed portion at the outlet the number of lines become lower and takes the parallel shape to the vertical wall. The lower number of pressure lines indicate the lower pressure. Due to the change of magnetic field strength from 0 to 12 tesla the pressure lines at the inlet portion changes their shapes from straight lines to parabolic lines which indicates higher pressure but after the stenosed portion the lines remain almost similar that indicates at the outlet portion the pressure remains lower with the change of magnetic field strength.

Figure 4.9. displays the viscosity countour for the considered magnetic field strength variation. Maximum viscosity of blood exists at the middle part of the stenosis due to the contraction of the domain. When the magnetic field strength changes from 0 to 2 tesla the viscosity at the middle of the stenosed portion increases slightly. There is a little bit change noticed in viscosity contour for higher magnetic field strength.

Figure 4.10(a-b) depicts the cross sectional plot of velocity magnitude and viscosity versus arc length at the middle of the stenosed part, respectively. The velocity profile is exactly parabolic. From this figure it is clearly seen that, maximum velocity magnitude at the cross sectional line is found about 0.038 m/s due to the stenosis. There is less difference in cross sectional plot for different magnetic field strength. In the Figure 4.10(b) the shear rate across the stenotic contraction is not exactly parabolic it is slightly distorted. For different magnetic field strength the cross-sectional plot of shear rate is almost similar and there are slight changes which are negligible.

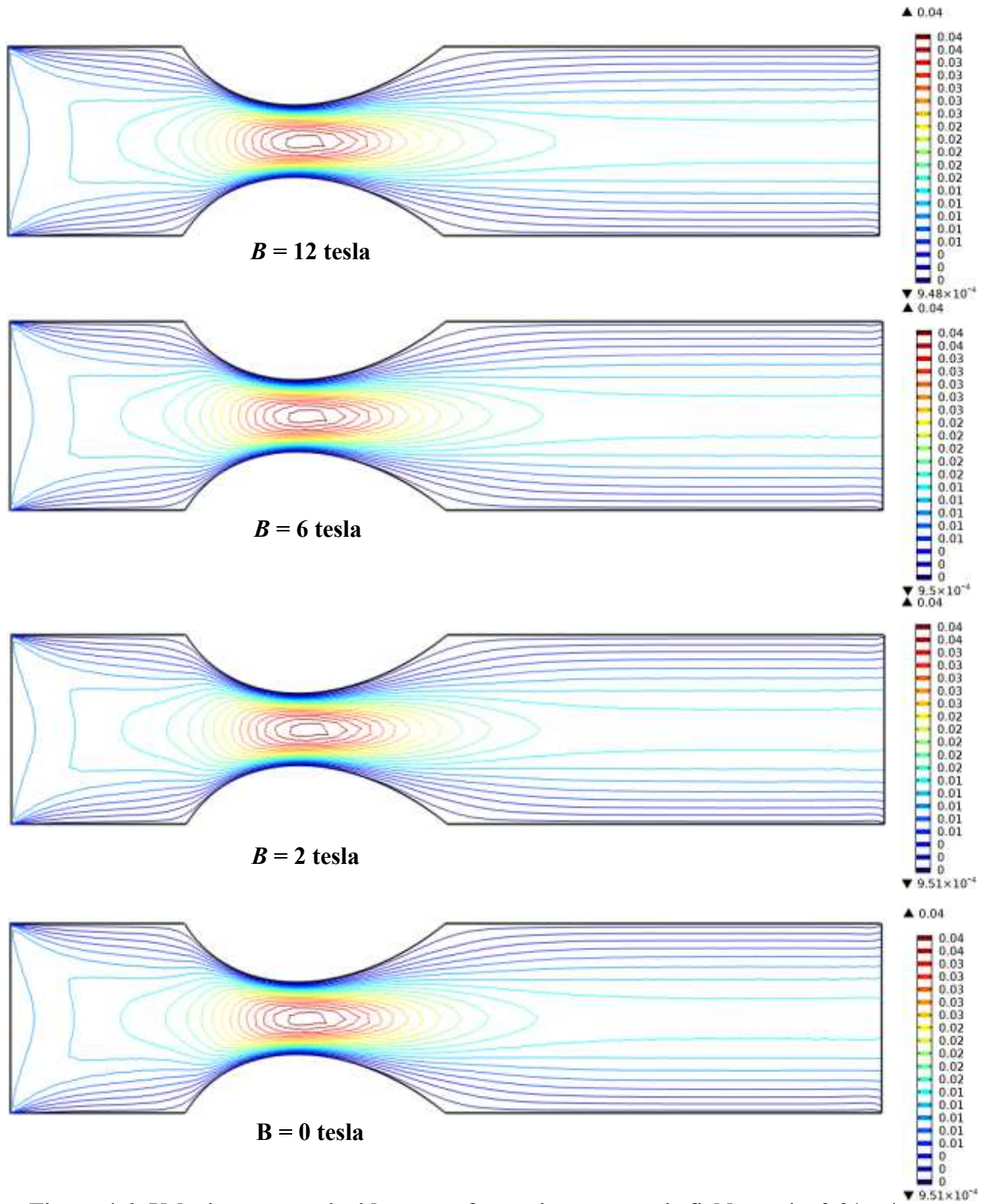


Figure 4.6: Velocity contour inside artery for various magnetic field at $u_i = 0.01$ m/s

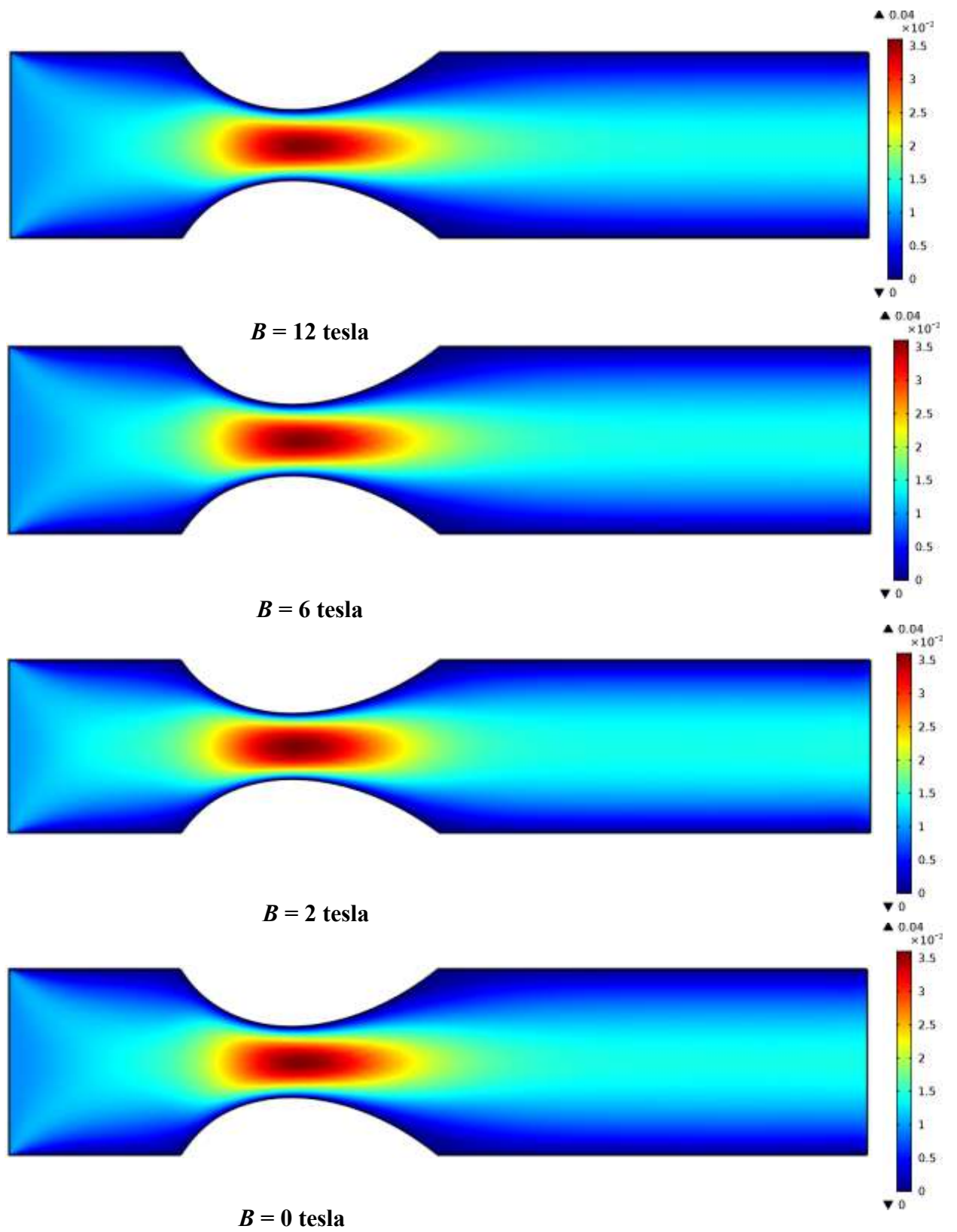


Figure 4.7: Surface plot of velocity magnitude artery for various magnetic field at $u_i = 0.01$ m/s.

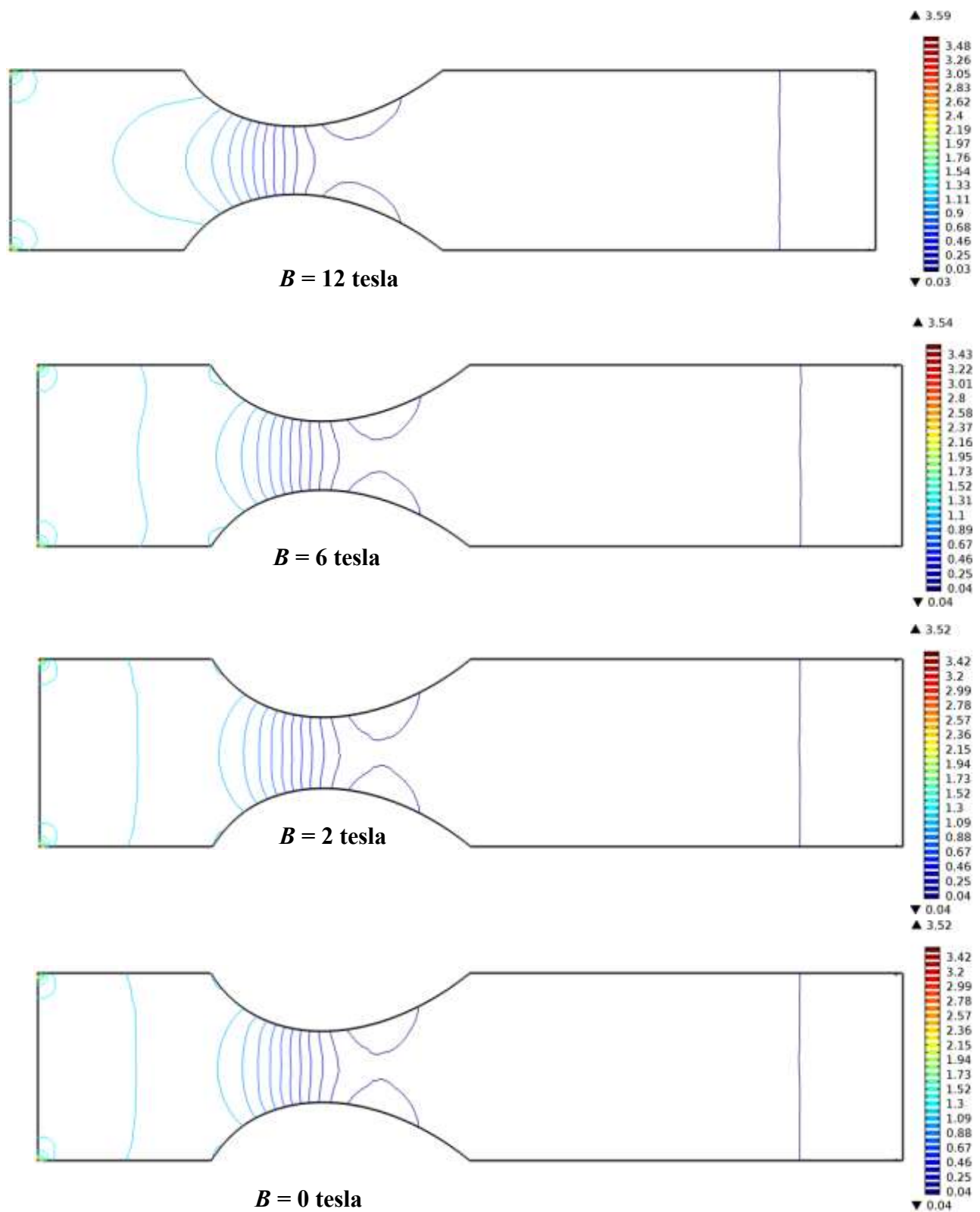


Figure 4.8: Pressure contour inside artery for various magnetic field at $u_i = 0.01$ m/s

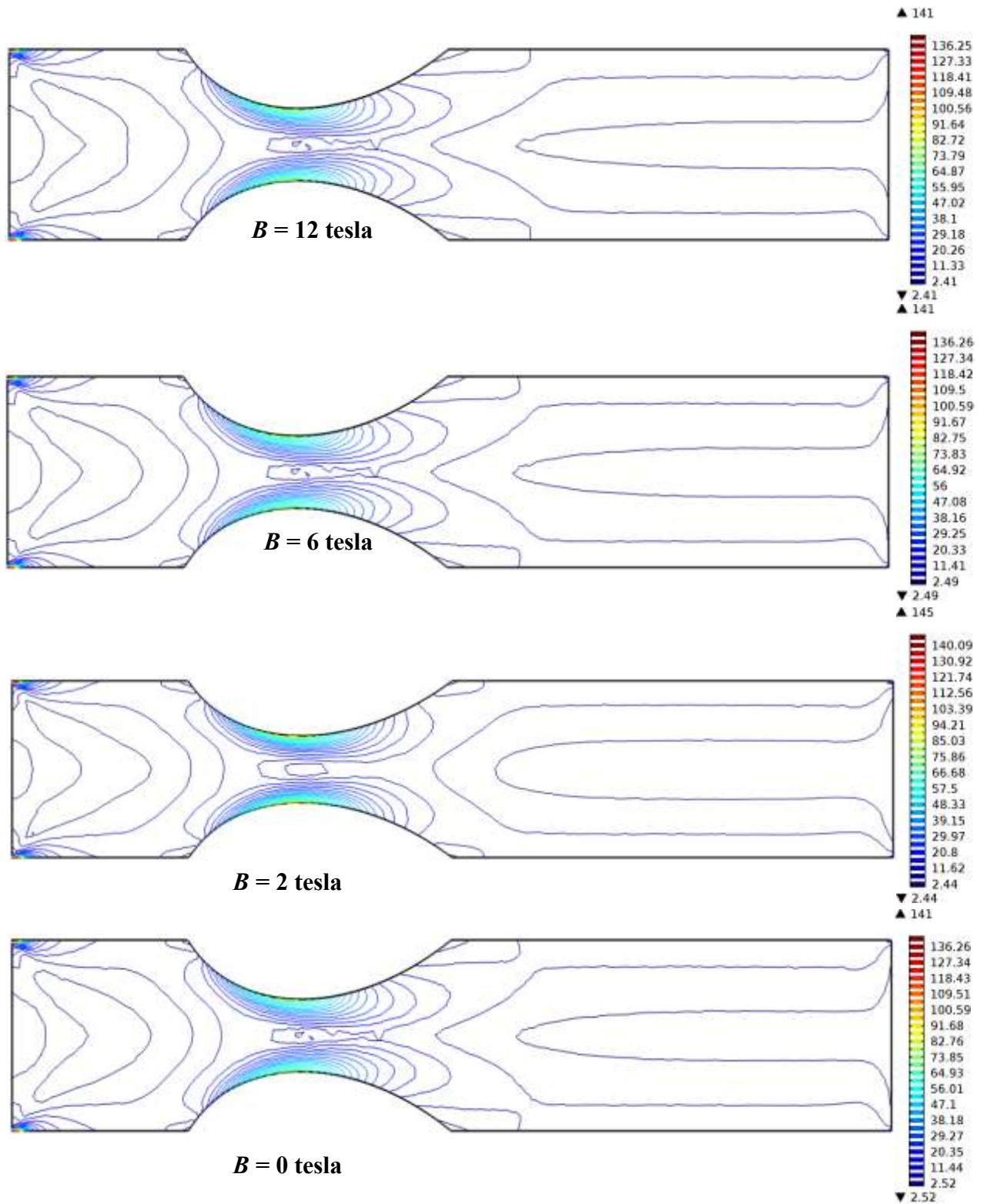
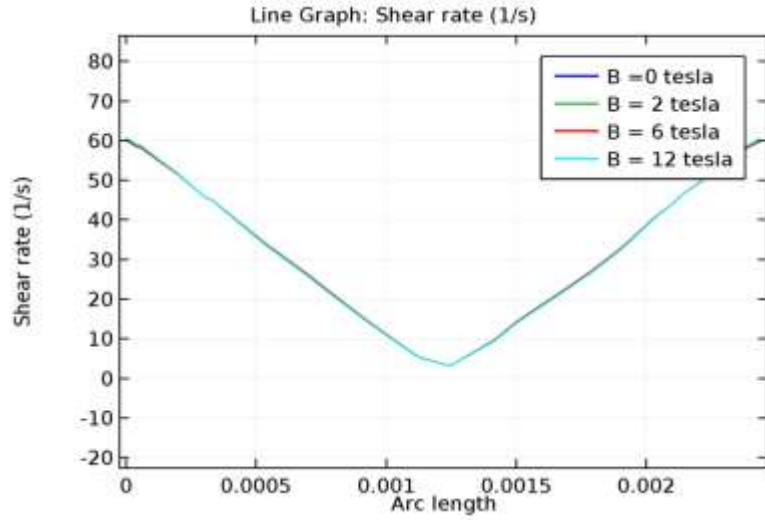
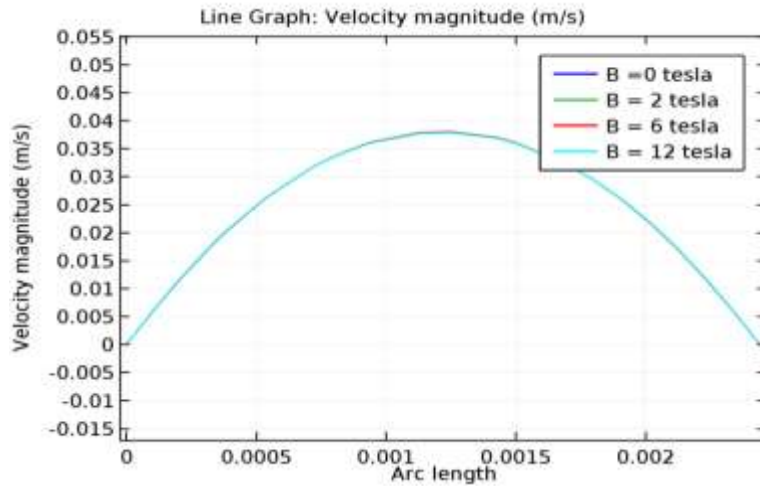


Figure 4.9: Viscosity contour of artery for various magnetic field at $u_i = 0.01$ m/s



(b)



(a)

Figure 4.10: Cross-sectional plot of (a) velocity magnitude and (b) shear rate for magnetic field variation across the stenotic contraction

CHAPTER 5: CONCLUSION AND RECOMMENDATIONS

A numerical study of controlling blood flow through a stenosed artery using Power-law fluid model has been conducted in the present research. Using the Galerkin's weighted residual finite element technique the governing equations have been solved. The effect of inlet blood velocity from 0.005 to 0.1 m/s on sub-domain velocity, surface, pressure and viscosity contours have been studied in detail in a stenosed artery. The imposed magnetic field strength has been considered from 0 to 12 tesla. In view of these arguments, the present study may be useful to control the blood flow in diseased state. From the present investigation the following conclusions may be drawn:

5.1 Conclusions

- Higher velocity and pressure are observed near the stenosed area.
- The high blood inlet velocity is responsible for lower pressure.
- Shear rate of blood increases due to increasing inlet velocity.
- The magnitude of velocity decreases with the increase of magnetic field.
- Increasing magnetic field strength increases the pressure of blood.
- Shear rate also increases for rising values of magnetic field.

5.2 Recommendations

The future research can be done considering the following proposals:

- This research may be extended including a mechanical analysis of the deformation of the tissue and artery with applying magnetic field on different directions.
- The next work will be devoted to an extension of this numerical study to unsteady blood flow and fluid-structure interaction model in stenotic and aneurismatic vessels, to provide a deeper understanding of the significance of the non-Newtonian characteristics of blood and its correlation with the cardiovascular diseases like atherosclerosis.

- The study can be extended for non-uniform blood vessel with different blood flow rates.
- In the future, the study can be extended by dissimilar physics like bending artery, vertical artery and cross-sectional artery and arterial bifurcation effects on blood flow.
- The simulation and mathematical properties of the blood flow for the model in the case of incompressible flow has been studied, but their performance may change for compressible flows. Therefore, this remains for future investigation.

REFERENCES

- [1] Razavi, A., Shirani, E. and Sadeghi, M.R., "Numerical simulation of blood pulsatile flow in a stenosed carotid artery using different rheological models", *J. of Biomechanics*, Vol. 44, pp. 2021-2030, 2011.
- [2] Shah, S.R., "An innovative study for non-Newtonian behaviour of blood flow in stenosed artery using Herschel-Bulkley fluid model", *Int. J. of Bio-science and Bio-Technology*, Vol. 5, No. 5, pp. 233-240, 2013.
- [3] Akbar, N.S. and Nadeem, S., "Carreau fluid model for blood flow through a tapered with a stenosis artery", *Ain Shams Engineering J.*, Vol. 5, pp. 1307-1316, 2014.
- [4] Singh, S. and Shah, R.R., "A numerical model for the effect of stenosis shape on blood flow through an artery using power-law fluid", *Advances in Applied Science Research*, Vol. 1, No 1, pp. 66-73, 2010
- [5] Tanwar, V.K., Varshney, N.K., and Agarwal, R., "Effect of body acceleration on pulsatile blood flow through a catheterized artery", *Advances in Applied Science Research*, Vol. 7, No. 2, pp. 155-166, 2016.
- [6] Singh, B., Joshi, P., and Joshi, B. K., "Blood flow through an artery having radially non-symmetric mild stenosis", *Applied Mathematics Science*, Vol. 4, pp. 1065-1072, 2010.
- [7] Steinman, D.A., Vorp, D.A., and Ethier, C.R., "Computational modeling of arterial biomechanics: insights into pathogenesis and treatment of vascular disease", *J. of Vascular Surgery*, Vol. 37, pp. 1118-1128, 2003.
- [8] Ismail, Z., Abdullah, I., Mustapha, N., Amin, N., "The power law model of blood flow through a tapered overlapping stenosed artery", *Applied Mathematics Comput.*, Vol. 195, pp. 669-680, 2008.
- [9] Hasan, T.A.B.M., Das, D.K., "Numerical simulation of sinusoidal fluctuated pulsatile laminar flow through stenotic artery", *J. of Applied Fluid Mechanics*, Vol.1, No. 2, pp. 25-35, 2008.

- [10] Akbar, N.S., "Blood flow analysis of Prandtl fluid model in tapered stenosed arteries", *Ain Shams Engineering J.*, Vol. 5, pp. 1267-1275, 2014.
- [11] Madadelahi, M., Shamloo, A., "Newtonian and generalized Newtonian reacting flows in serpentine microchannels: Pressure driven and centrifugal microfluidics", *J. of Non-Newt. Fluid Mech.*, Vol. 251, pp. 88-96, 2018.
- [12] Uddin, M.N. and Alim, M.A., "Numerical investigation of blood flow through stenotic artery", *World J. of Engineering Research and Technology*, Vol. 3, Issue 6, pp. 93-116, 2017.
- [13] Bali, R. and Awasthi, U., "A Casson fluid model for multiple stenosed artery in the presence of magnetic field", *Applied Mathematics*, Vol. 3, pp. 436-441, 2012.
- [14] Rahman, M.M., Hossain, M.A., Mamun, K. and Akhter, M.N., "Comparative study of Newtonian and non-Newtonian blood flow through a stenosed carotid artery", *AIP Conf. Proc.*, 1980, 040017 (2018); doi: 10.1063/1.5044327.
- [15] Nadeem, S., Akbar, N.S., Hendi, A.A., Hayat, T., "Power-law fluid model for blood flow through a tapered artery with a stenosis", *Applied Maths. And Comp.*, Vol. 217, pp. 7108-7116, 2011.
- [16] Long, Q., Xu, X.Y., Ramnarine, K.V., Hoskins, P., "Numerical investigation of physiologically realistic pulsatile flow through arterial stenosis", *J. of Biomechanics*, Vol. 34, pp. 1229-1242, 2001.
- [17] Abdel Baieth, H.E., "Physical parameters of blood as a non-Newtonian fluid", *Int. J. of Biomedical Science*, Vol. 4, No. 4, pp. 323-329, 2008.
- [18] Peskin, C.S., "Numerical analysis of blood flow in the heart", *J. Computational Physics*, Vol. 25, pp. 220-252, 1977.
- [19] Kumar, S. Diwakar, C., "A mathematical model of Power law fluid with an application of blood flow through an artery with stenosis", *Advances in Applied Mathematical Biosciences*, Vol. 4, No. 2, pp. 51-61, 2013.
- [20] Chandra, S. and Singh, P., "Effects of stenosis on Power law fluid flow of blood in blood vessels", *Journal for Research*, Vol. 01, Issue 09, 2015.

- [21] Imaeda, K. and Goodman, F.O., "Analysis of nonlinear pulsatile blood flow in arteries", *J. of Biomechanics*, Vol. 13, No. 12, pp. 1007-1021, 1980.
- [22] Srivastava, V.P., "Particular suspension blood flow through stenotic arteries: effect of hematocrit and stenosis shape", *Indian J. Pure Applied Mathematics*, Vol. 33, No.9, pp. 1353-1360, 2002.
- [23] Ponalagusamy, R., "Blood flow through an artery with mild stenosis: A two layered model, different shapes of stenosis and slip velocity at the wall", *J. of Applied Sciences*, Vol. 7, No. 7, pp. 1071-1077, 2007.
- [24] Srivastava, V.P. and Saxena, M., "Two-layered model of casson fluid flow through stenotic blood vessels applications to the cardiovascular system", *J. of Biomechanics*, Vol. 27, No. 7, pp. 921-928, 1994.
- [25] Thurstan, G.B., "Viscoelasticity of human blood", *Biophysical J.*, Vol. 12, pp. 1205-1217, 1972.
- [26] Sankar, D.S. and Hemalatha, K., "Pulsatile flow of Herschel-Bulkley fluid through stenosed arteries-A mathematical model", *Int. J. of Non-Linear Mechanics*, Vol. 41, No. 8, pp. 979-990, 2006.
- [27] Chakravarty, S. and Mandal, P.K., "Two-dimensional blood flow through tapered arteries under stenotic conditions", *Int. J. of Non-Linear Mechanics*, Vol. 35, No. 5, pp. 779-793, 2000.
- [28] Leuprecht, A. and Perktold, K., "Computer simulation of non-newtonian effects on blood flows in large arteries", *Computer Methods in Biomech. & Biomedical Engg.*, Vol. 4, pp. 149-163, 2001.
- [29] Srivastav, R.K. and Agnihotri, A.K., "Non-Newtonian power-law blood fluid flow through bell-shaped stenosis artery", *J. of Multidisciplinary Scientific Research.*, Vol. 2, No. 4, pp. 15-19, 2014.
- [30] Shahidian, A., Hassemi, M., Khorasanizade, S., Abdollahzade, M., and Ahmadi, G., "Flow analysis of non-Newtonian blood in a magneto hydrodynamic pump", *IEEE Transactions on Magnetics*, Vol. 45, pp. 2667-2670, 2009.

- [31] Haldar, K., "Effects of the shape of stenosis on the resistance to blood flow through an artery", *Bulletin of Mathematical Biology*, Vol. 47, pp. 545-550, 1985.
- [32] Mathur, P. And Jain, S., "Mathematical modelling of non-Newtonian blood flow through artery in the presence of stenosis", *Advances in Applied Mathematical Biosciences*, Vol. 4, pp. 1-12, 2013.
- [33] Tzirtzilakis, E., "A mathematical model for blood flow in magnetic field", *Physics of Fluids*, Vol. 17, pp. 077-103, 2005.
- [34] Mandal, P.K., "An unsteady analysis of non-Newtonian blood flow through tapered arteries with a stenosis", *Int. J. of Non-Linear Mechanics*, Vol. 40, No.1, pp. 151-164, 2005.
- [35] Mantha, A.R., Benndorf, G., Hernandez, A., Metcalfe, R.W., "Stability of pulsatile blood flow at the ostium of cerebral aneurysms", *J. of Biomechanics*, Vol. 42, pp. 1081-1087, 2009.
- [36] Mekheimer, Kh.S. and Kot, M.A.E., "The micropolar fluid model for blood flow through a tapered artery with a stenosis", *Acta Mechanica Sinica*, Vol. 24, No. 6, pp. 637-644, 2008.
- [37] Shukla, J.B., Parihar, R.S. and Rao, B.R.P., "Effects of stenosis on non-Newtonian flow of the blood in an artery", *Bulletin of Mathematical Biology*, Vol. 42, pp. 283-294, 1980.
- [38] Hershey, D., Byrnes, R.E. and Roam, A.M., "Blood rheology: temperature dependent of the Power-law model", *A.I.C.H. Meeting*, Boston, 1964.
- [39] Taylor, C. Hood, P., "A numerical solution of the Navier-Stokes equations using finite element technique", *Computer and Fluids*, Vol. 1, pp. 73-89, 1973.
- [40] Dechaumphai, P., "Finite Element Method in Engineering", 2nd edition, Chulalongkorn University Press, Bangkok, 1999.
- [41] <https://science.howstuffworks.com/question698.htm>